

## **Understanding nitrate formation in a world with less sulfate.**

1

Petros Vasilakos<sup>1</sup>, Armistead Russell<sup>2</sup>, Rodney Weber<sup>3</sup>, and Athanasios Nenes<sup>1,3,4,5†</sup>

<sup>1</sup> School of Chemical and Biomolecular Engineering, Georgia Institute of Technology, Atlanta, Georgia, 30332, USA

<sup>2</sup> School of Civil and Environmental Engineering, Georgia Institute of Technology, Atlanta, Georgia, 30332, USA

<sup>3</sup> School of Earth and Atmospheric Sciences, Georgia Institute of Technology, Atlanta, Georgia, 30332, USA

<sup>4</sup> Institute of Chemical Engineering Sciences, Foundation for Research and Technology-Hellas, Patras, GR 26504, Greece

<sup>5</sup> Institute for Environmental Research and Sustainable Development, National Observatory of Athens, Palea Penteli, GR 15236, Greece

†Corresponding Author: A. Nenes ([athanasios.nenes@gatech.edu](mailto:athanasios.nenes@gatech.edu))

2

## Abstract

3           SO<sub>2</sub> emission controls, combined with modestly increasing ammonia, have been thought  
4 to generate aerosol of significantly reduced acidity where sulfate is partially substituted by nitrate.  
5 However, neither expectation agrees with decadal observations in the Southeastern US, suggesting  
6 that a fundamentally different response of aerosol pH to emissions changes is occurring. We  
7 postulate this “nitrate substitution paradox” arises from a positive bias in aerosol pH in model  
8 simulations. This bias can elevate pH to where nitrate partitioning is readily promoted, leading to  
9 behavior consistent with “nitrate substitution”. CMAQ simulations are used to investigate this  
10 hypothesis; modeled PM<sub>2.5</sub> pH using 2001 emissions compare favorably with pH inferred from  
11 observed species concentrations. Using 2011 emissions, however, leads to simulated pH increases  
12 of one unit, which is inconsistent with observations from that year. Non-volatile cations (K<sup>+</sup>, Na<sup>+</sup>,  
13 Ca<sup>+2</sup>, and Mg<sup>+2</sup>) in the fine mode are found responsible for the erroneous predicted increase in  
14 aerosol pH of about 1 unit on average over the US. Such an increase can induce a nitrate bias of  
15 1-2 μg m<sup>-3</sup> which may further increase in future projections, reaffirming an otherwise incorrect  
16 expectation of a significant “nitrate substitution”. Evaluation of predicted aerosol pH against  
17 thermodynamic analysis of observations is therefore a critically important, but overlooked, aspect  
18 of model evaluation for robust emissions policy.

19

## 20 **Introduction**

21 Aerosol acidity is a driver of many important atmospheric processes (Guo et al. 2015,  
22 Weber et al. 2016), catalyzing the conversion of isoprene oxidation products to form secondary  
23 organic aerosol (SOA) (Xu et al. 2015, Pye et al. 2013, Surratt et al. 2010, Eddingsaas et al. 2010)  
24 and driving the semi-volatile partitioning of key aerosol species (Guo et al. 2015, Weber et al.  
25 2016). High acidity can also lead to the solubilization of iron, copper and other trace metals in  
26 aerosol which may serve as nutrients for ecosystems (Meskhidze et al. 2003), but also prove toxic  
27 for humans (Ghio et al. 2012, Fang et al. 2017). Significant reductions in primary pollutant  
28 emissions over the last decades has greatly improved air quality in the developed world, and is  
29 also thought to fundamentally affect aerosol acidity. SO<sub>2</sub>, an important aerosol precursor and a  
30 major driver of its acidity, has seen decreases of about 6% yr<sup>-1</sup> over the 2001-2011 period alone  
31 in the US, with a continued anticipated downward trend (Pinder et al. 2007, 2008). Emissions of  
32 NO<sub>x</sub> and the resulting acidic HNO<sub>3</sub>, are also declining. In contrast, ammonia, the primary alkaline  
33 fine mode aerosol precursor, was either constant or increasing during this period (Pinder et al.  
34 2007, 2008, Heald et al. 2012), owing to intensified agricultural activity and livestock farming  
35 from the demands of population growth. These trends have created the expectation that the aerosol  
36 has and will become increasingly less acidic (West et al. 1999, Pinder et al. 2007, 2008, Heald et  
37 al. 2012, Tsimpidi et al. 2007, Saylor et al. 2015), with ammonium sulfate being replaced, at least  
38 in part, by ammonium nitrate (West et al. 1999, Bauer et al. 2007, Bellouin et al. 2007, Li et al.  
39 2014, Goto et al. 2016).

40 The concept of “nitrate substitution” of sulfate has largely been based on the notion that  
41 nitrate is volatile when the aerosol is acidic, and in turn aerosol is acidic when insufficient amounts  
42 of total ammonia (i.e., gas+aerosol) or dust non-volatile cations (NVCs) exist to neutralize aerosol  
43 sulfate. Based on this conceptual model, aerosol ionic molar ratios have largely been used as  
44 proxies of aerosol acidity (pH), so that when the aerosol ammonium to sulfate molar ratio  
45 approaches 2 (the composition of ammonium sulfate), aerosol is assumed “neutral” and only then  
46 nitrate aerosol can form (Fisher et al. 2011, Hennigan et al. 2015, Wang et al. 2016, Silvern et al.  
47 2017). Modeling studies have corroborated this view, predicting that nitrate substitution may be  
48 prevalent in the future, including the Southeastern US (SE US) (Heald et al. 2014, Baeur et al.  
49 2007, Bellouin et al. 2011, Li et al. 2014, Goto et al. 2016, Vayenas et al. 2005, Karydis et al.  
50 2016). A more careful analysis however (Guo et al. 2015, Weber et al. 2016, Hennigan et al. 2015,

51 Guo et al. 2016) reveals that this conceptual model of aerosol acidity and conditions for nitrate  
52 substitution fail; thermodynamic analysis of SE US aerosol observations instead show that fine  
53 mode aerosol remains strongly acidic, despite a 70% reduction in sulfates, and more than sufficient  
54 total ammonia to neutralize it. The strong acidity is maintained by the large difference in volatility  
55 between sulfate and ammonia (Guo et al. 2015, Weber et al. 2016), so large changes in total  
56 ammonia concentrations are required for a notable change in aerosol acidity, about one order of  
57 magnitude increase in  $\text{NH}_3$  concentration per unit increase in aerosol pH (Guo et al. 2015 &  
58 2017c). However, ammonia gas deposits relatively rapidly, limiting its build up except in high  
59 emissions regions. Throughout the decade, the levels of aerosol nitrate have remained relatively  
60 constant throughout the US (Guo et al. 2015, Weber et al. 2016, Pye et al. 2009). The persistent  
61 strong aerosol acidity in turn explains why nitrate aerosol has not considerably increased over the  
62 last decades, and is unlikely to appear in the immediate future in the SE US. These findings  
63 constitute a “paradox”, as the same thermodynamic models (e.g., ISORROPIA-II Fountoukis &  
64 Nenes 2007) used to demonstrate the aerosol tendency for strong acidity in the SE US (Guo et al.  
65 2015, Weber et al. 2016) using ambient data, is also used in 3D modeling studies (Pye et al. 2009,  
66 Heald et al. 2012) for the region that predict nitrate substitution as a possible aerosol response.

67 Reconciling the “nitrate substitution paradox” requires a careful examination of aerosol  
68 thermodynamics and the conditions under which nitrate partitioning to the aerosol is favored.  
69 Meskhidze et al. (2003) and later Guo et al. (2016) showed that for aerosol nitrate formation to  
70 occur, aerosol pH needs to exceed a certain characteristic value (that depending on the temperature  
71 and the amount of liquid water, ranges between a pH of 1.5 and 3; Guo et al., 2017). If aerosol pH  
72 is therefore high enough (typically above a pH of 2.5 to 3), a behavior consistent with “nitrate  
73 substitution” emerges, because any inorganic nitrate forming from  $\text{NO}_x$  chemistry mostly resides  
74 in the aerosol phase. When pH is low enough (typically below 1.5 to 2), nitrate remains exclusively  
75 in the gas phase (as  $\text{HNO}_3$ ), regardless of the amount produced, and “nitrate substitution” is not  
76 observed. Between these “high” and “low” pH values, a “sensitivity window” emerges (of  
77 typically 1-1.5 pH units), where partitioning shifts from nitrate being predominantly found as gas  
78 to where it is mostly found as an aerosol. Therefore, if a model is for any reason biased in its  
79 prediction of aerosol pH, it may be preconditioned towards nitrate prediction biases. The  
80 sensitivity to pH biases is strongest when the aerosol lies in the pH “sensitivity window”, which  
81 is often the case for atmospheric aerosol (Guo et al. 2015, 2016 & 2017, Bougiatioti et al. 2016).

82 When below this “pH sensitivity window”, aerosol nitrate is almost nonexistent and relatively  
83 insensitive to emissions (and pH biases); when above the window, almost all nitrate resides in the  
84 aerosol phase, and directly responds to NO<sub>x</sub> emission controls.

85 If aerosol were composed only of non-volatile sulfate and semi-volatile nitrate and  
86 ammonium, prediction biases in pH could result only from errors in RH, and large errors (e.g.,  
87 order of magnitude) of NH<sub>3</sub>, NO<sub>x</sub> and SO<sub>2</sub> because pH is relatively insensitive to changes in these  
88 aerosol precursors (Hennigan et al. 2015). Acidity however can also be modulated by other soluble  
89 inorganic cations from seasalt and mineral dust, such as K<sup>+</sup>, Na<sup>+</sup>, Ca<sup>+2</sup> and Mg<sup>+2</sup>. The low volatility  
90 of these cations allows them to preferentially neutralize sulfates over NH<sub>3</sub>, and, even in small  
91 amounts elevate particle pH to levels that can promote the partitioning of nitrates to the aerosol  
92 phase (Fountoukis & Nenes 2007, Guo et al. 2017a). NVCs tend to reside in the coarse mode  
93 aerosol, with a fraction found in smaller particles, while sulfate tends to reside in the fine mode  
94 (e.g., West et al. 1999, Vayenas et al. 2005, Guo et al. 2015); the degree to which NVCs can affect  
95 fine mode pH therefore lies in the degree to which the two types of species mix across different  
96 particle sizes. Potential interactions between inorganics-organics can also affect aerosol acidity.  
97 However, recent studies driving thermodynamic models utilizing water associated with organics  
98 find only minimal differences in pH predictions (Guo et al. 2015, Bougiatioti et al. 2016, Liu et  
99 al. 2017, Pye et al., 2018, Song et al. 2018). In the presence of very high NVCs (for example in  
100 sea-spray aerosol), where the aerosol has much higher pH, the pH can approach the pK<sub>a</sub> of organic  
101 acids, leading to conditions where their dissociation can contribute to aerosol acidity (Laskin et  
102 al. 2012).

103 Although aerosol models are evaluated in terms of their ability to predict the concentration  
104 of aerosol species (including across size), no studies to date focus on their ability to predict aerosol  
105 pH across size, even though it is known to potentially vary up to 6 units (Fang et al. 2017,  
106 Bougiatioti et al. 2016, Li et al. 2017). Evaluation of models in this context is challenging, since  
107 there is no established dataset of aerosol acidity - although that is rapidly changing, with pH  
108 estimates derived from a combination of observations and models (e.g., Guo et al., 2015;  
109 Bougiatioti et al., 2016; Guo et al., 2017; Liu et al., 2017; Song et al., 2018) -. Furthermore, given  
110 that most of this pH variability occurs in the PM<sub>1</sub> to PM<sub>2.5</sub> range (Fang et al. 2017), it is quite  
111 likely that model assumptions on how aerosol species interact within a mode (degree of internal

112 mixture), especially for particles in the 1-2.5  $\mu\text{m}$  range, may lead to pH prediction biases that drive  
113 model behavior.

114 This aim of this study is to address the underlying reasons for the “nitrate substitution”  
115 paradox, and in the process, provide a conceptual framework for quantifying and understanding  
116 the importance of aerosol pH biases. The guiding hypothesis of this work is that aerosol pH  
117 prediction bias fundamentally changes predicted aerosol behavior and is the underlying cause of  
118 the paradox. The approach is demonstrated with the Community Multiscale Air Quality (CMAQ)  
119 model (Byun & Schere 2006) and is based on predictions of pH over the 2001-2011 period in the  
120 Southeastern/Eastern US, being the region for which aerosol pH trends are constrained by  
121 observations. The role of internally-mixed nonvolatile cations in  $\text{PM}_{2.5}$  as a source of the pH bias  
122 is then assessed.

123

## 124 **Methods**

### 125 **Predicting aerosol pH and composition**

126 CMAQ is a three-dimensional, Eulerian, atmospheric chemistry and transport model, that  
127 simulates the processes atmospherically relevant compounds undergo, such as emission, diffusion,  
128 chemical reactions and deposition (Byun & Schere 2006). CMAQ version 5.0.2 was used in this  
129 study, and simulations were carried out using a 36-km horizontal resolution grid, with 13 vertical  
130 layers, over the continental US (CONUS) for the entire years of 2001 & 2011. Meteorological  
131 data were obtained offline from the Weather Research Forecasting (WRF) model. The same  
132 meteorology was used between the two years to eliminate the effect of differences due to  
133 temperature and relative humidity on pH predictions.. Model-ready emissions for 2011 were  
134 obtained using the National Emissions Inventory 2011 inventory (NEI 2011) for the Carbon Bond  
135 05 (CB05) chemical mechanism. To estimate the 2001 emissions, the 2011 emissions for  $\text{SO}_2$ ,  
136  $\text{NO}_x$ ,  $\text{NH}_3$ , CO, VOCs and primary PM from anthropogenic sources were scaled on a per-species  
137 basis using the Air Pollutant Emissions Trends Data (2017); emissions for other species were kept  
138 constant. Specifically anthropogenic CO,  $\text{NO}_x$ , primary PM and  $\text{SO}_2$  emissions were increased by  
139 44%, 45%, 15% and 246% respectively, while VOC and  $\text{NH}_3$  emissions were reduced by 6% and  
140 14% respectively. Emissions of biogenic species were calculated online using the Biogenic  
141 Emission Inventory System (BEIS).

142 The aerosol thermodynamic model ISORROPIA-II (subversion 2.1 - dated 2008 –  
143 Fountoukis & Nenes 2007) was used online in CMAQ to drive the semivolatile partitioning of  
144 inorganic species, as well as offline to analyze the predicted PM<sub>2.5</sub> pH, nitrate partitioning  
145 tendency and sensitivities thereof to nonvolatile cations. It should be noted that ISORROPIA and  
146 CMAQ only account for the thermodynamic interactions between inorganic species and do not  
147 treat organics. Offline calculations were conducted using the hourly gas and particle phase  
148 concentrations output from CMAQ for the 2001 and 2011 simulations, which includes NVCs, and  
149 using them as input to ISORROPIA-II (subversion 2.3 - dated 2012). The thermodynamic  
150 calculations online and offline were carried out in forward mode, meaning that the temperature,  
151 relative humidity, as well as all aerosol and gas phase concentrations were known and used as  
152 input, while at the same time assuming that the aerosol is in a metastable state, where only one  
153 aqueous phase is allowed to exist (Fountoukis & Nenes 2007). This assumption is not always  
154 necessarily true, especially under conditions of low relative humidity (RH<30%) where the aerosol  
155 can crystalize or exist in glassy, amorphous state (where in this case thermodynamic equilibrium  
156 is not reached), observational data of liquid water content shows that it is most often a valid  
157 assumption (Guo et al. 2015, Bougiatioti et al. 2016), and other studies suggest that the phase state  
158 may not strongly affect predicted pH (Song et al., 2018). We run the model under a variety of  
159 conditions to determine the impact of NVCs from dust and sea salt (Ca, Mg, K, Na) on pH, its  
160 seasonal variability, as well as the effect of pH and temperature on nitrate partitioning.

161

## 162 **Results and discussion**

### 163 **Predicted Sulfate, ammonium & nitrate**

164 For the main inorganic aerosol species (SO<sub>4</sub><sup>2-</sup>, NO<sub>3</sub><sup>-</sup> and NH<sub>4</sub><sup>+</sup>), CMAQ captures the  
165 observed trends, as seen in the literature (Park et al. 2006, Hand et al. 2012, Blanchard et al. 2013a,  
166 b, Kim et al. 2015, Saylor et al. 2015) over the CONUS over the course of the decade (Figure S1).  
167 As expected, sulfate over the entire US drops significantly between 2001 and 2011 (~ 30%), with  
168 major decreases in the Eastern US (~2 μg m<sup>-3</sup>). Areas impacted the most by these reductions are  
169 places of significant industrial activity or coal-fired electricity generating units (EGUs), such as  
170 the Ohio River Valley, Baton Rouge in Louisiana and South Carolina. Ammonium levels only  
171 experience small reductions which are a buffered response to the decrease in sulfate levels, and  
172 minimal changes in emissions. Local reductions (~20%) in ammonia are seen over North Carolina

173 and Louisiana. Aerosol nitrate concentrations remain constant on average over the domain, with  
174 small increases over the Eastern US. The highest levels of ammonium are observed in areas with  
175 significant livestock, such as North Carolina and the Midwest; sulfate concentrations are the  
176 highest around the Ohio River Valley, due to  $\text{SO}_x$  emissions, and so is nitrate due to significant  
177  $\text{NO}_x$  and ammonia emissions.

178

### 179 **Predicted Annual & seasonal pH**

180 Figure 1 depicts the annual average pH fields over the US for 2001 and 2011, calculated  
181 using the annual average  $\text{PM}_{2.5}$  concentrations, with the study domain of the Eastern US outlined.  
182 Simulations show that there are noticeable differences between the two years, localized mainly in  
183 desert regions along the US-Mexico border, Southern Texas and the Eastern US. The sulfate  
184 reductions in the Eastern US, appear to have a major impact on model results, leading to significant  
185 increases of aerosol pH in the area. For 2001, the average yearly pH for the Eastern US is 1.6,  
186 consistent with recent literature and observations from the WINTER campaign (Guo et al. 2015  
187 & 2016, Weber et al. 2016) (Figure 1a). For 2011, however, predicted pH increases to about 2.5 –  
188 almost a unit higher (Figure 1b).

189 Seasonal pH trends are also positive over the Eastern US, with the summertime (Figure  
190 S2f) experiencing stronger increases than in the winter (Figure S2c), being 0.5-1.5 for winter and  
191 0.5-2 for summer. Much of the seasonal variability is driven by changes in temperature and relative  
192 humidity; increased relative humidity (RH) leads to less acidic aerosol, since liquid water content  
193 and pH are inversely related (Guo et al. 2015 & 2016), while increased temperatures promote low  
194 RH and therefore more acidic aerosol. The desert areas of the Western US, Southern Texas,  
195 Florida, SW Alabama and Mississippi are the most sensitive in the wintertime (Figure S2a, b),  
196 while the Central US is mostly unaffected. During the summer, the entire Central US is much  
197 more strongly impacted, while the wintertime sensitive areas exhibit only minor pH increases  
198 (Figure S2d, e).

### 199 **Model evaluation of pH**

200 Model results for both simulation years were compared to thermodynamic analysis of  
201 measurements from three urban sites in Atlanta, Georgia (Jefferson Street, JST; Georgia Tech,  
202 GT; Atlanta Road-Side, RS) and two rural (Yorkville, Georgia - YRK; and Centerville, Alabama  
203 - CTR) SEARCH network sites. Measurements for the urban sites and the YRK site, were taken



204 between May and December 2012 for the SCAPE study, while measurements from the CTR site  
205 were for the SOAS campaign period (June 1<sup>st</sup> to July 15<sup>th</sup> 2013) (Guo et al. 2015, Xu et al. 2015).  
206 The three urban sites are contained within the same CMAQ grid cell. All urban sites (Figure 2a,  
207 b, c, d), exhibit an early morning/late night pH maximum, and an afternoon minimum throughout  
208 the year (Guo et al. 2015). This a combination of two factors; RH being highest during the early  
209 morning/late night, which increases water uptake and hence decreases acidity (Guo et al. 2015)  
210 (Figure S3), and the presence of crustal elements in significant quantities during that time (Figure  
211 S4). The model pH closely tracks the diurnal profile of predicted cations (Figure S4), indicating  
212 that they have an important impact on predicted pH, which, however, is not seen in the  
213 measurements (Figure 2), since they make up a much smaller percentage of observed PM<sub>2.5</sub>.  
214 Despite the presence of NVCs, the pH remains low for both simulation years but it tends to be  
215 higher in 2011, because of sulfate levels that are approximately half of those in 2001 across all  
216 sites, leading to the increased relative effect of NVCs (Weber et al. 2016). Removal of all NVCs  
217 from the thermodynamic calculations (Figure S5), significantly reduces the pH differences  
218 between 2001 and 2011 while removing some of the increased variability introduced by NVCs.  
219 At the same time, a negative bias is introduced to the simulated pH, which is more prominent for  
220 the urban sites even after the sulfate reductions.

221 The increase in pH is not proportional to the reduction in sulfate, since aerosol responds  
222 non-linearly to such reductions, through the volatilization of ammonia (Weber et al. 2016).  
223 Depending on location, sulfate reductions range from 38 to 55%, while the corresponding pH  
224 increase is much lower, pointing to the fact that cations, although small in amount, tend to have a  
225 disproportionately strong impact on acidity. For the SOAS campaign period (Figure 2g), pH is  
226 underestimated especially for 2001. The biases follow the pattern of NVCs present, by being  
227 negatively biased until noon and positively biased for the rest of the day (Figure 2 and Figure S4).  
228 The bias is particularly evident in the early morning hours where NVC concentrations reach a  
229 maximum (Figure S4). For the YRK site (Figure 2b, e), pH is overall underestimated during the  
230 winter and overestimated during the summer. Similarly to the urban sites, the predicted RH agrees  
231 well with the measurements (Figure S3), albeit with a positive afternoon bias during the summer.  
232 The diurnal profile of pH closely tracks the one of cations, further suggesting they may be directly  
233 related to the bias.

234           When evaluating the predicted pH trend for CTR, the model results exhibit a clear,  
235 increasing trend of 0.6 pH units per decade (Figure 3). This trend is inconsistent with recent  
236 thermodynamic analysis of observations suggesting a slight decrease in pH over the same time  
237 period for the SE US (Guo et al. 2015 & 2016, Weber et al. 2016). If this bias in predicted pH  
238 trend continues, it can have profound implications for future regulatory modeling, since the  
239 increased pH can lead to elevated levels of model nitrate, reproducing nitrate substitution (Bauer  
240 et al. 2007, Bellouin et al. 2011, Li et al. 2014, Goto et al. 2016). Possible reasons behind this pH  
241 bias could be overestimated ammonia emissions, underestimated sulfate, or, the presence of NVCs  
242 in PM<sub>2.5</sub>. The first two possibilities are unlikely, given the agreement of predicted ammonium and  
243 sulfate with previous studies (Park et al. 2006, Hand et al. 2012, Blanchard et al. 2013a, b, Kim et  
244 al. 2015, Saylor et al. 2015), and, the relative insensitivity of pH to ammonia and sulfate (Weber  
245 et al. 2016, Silvern et al. 2017). However, NVCs, if inappropriately distributed in PM<sub>2.5</sub>, can exert  
246 important biases on pH (Meskhidze et al. 2003, Karydis et al. 2016, Guo et al. 2017b). Indeed,  
247 offline calculations of aerosol pH excluding the influence of NVCs mitigates most of the predicted  
248 positive trend of 0.6 pH units per decade when all the aerosol species are considered (Figure 3),  
249 while also reducing standard error. The remaining bias may arise from errors in model RH, given  
250 that it controls water uptake and drives much of the diurnal variability in pH (Guo et al. 2015).  
251 Usage of observed (instead of predicted) RH in the thermodynamic calculations, did not impact  
252 the predicted pH more than 0.1 units (Figure S6). A more thorough evaluation of the remainder of  
253 the pH bias, as well as the impact of NVCs when included in appropriate quantities, requires a far  
254 more extensive analysis of the emissions profiles – especially regarding its diurnal variability -  
255 and observational dataset than the one available for this study (Henneman et al. 2017, Guo et al.  
256 2017c).

257           The pH bias becomes negative for most of the CMAQ Eastern US when removing all  
258 NVCs from the calculations (Figure S5). This, combined with the considerable model skill for  
259 sulfate, nitrate and ammonium when compared to literature (Henneman et al. 2017) implies that  
260 pH biases are not related to errors in the major inorganic ions or biases in meteorological  
261 parameters (humidity and temperature), but rather in the NVCs which are minor contributors to  
262 PM<sub>2.5</sub>, hence poorly constrained. For the SEARCH sites NVCs comprise 5 to 10% of the total  
263 inorganic PM<sub>2.5</sub> (Guo et al. 2015), which is significantly less than what the model predicted values  
264 that are a factor of 4 higher than the measurements. The most important result therefore is that

265 NVCs are a considerable source of pH prediction uncertainty when not accounted for correctly  
266 (Supplementary material: The role of NVCs in PM<sub>2.5</sub> pH). It should be noted that for the  
267 summertime at the CTR location, the ammonium and sulfate values are biased low in CMAQ by  
268 a factor of 3 using the Weber et al. 2016 data. These biases however are consistent with literature  
269 and typical of CTMs (Henneman et al 2017).

270 The SEARCH sites have been thoroughly studied in previous literature (Guo et al, 2015 &  
271 2017a, Xu et al. 2015, Weber et al. 2016) and given the high concentrations of organic mass  
272 observed throughout the year, they present an excellent case study for the potential impact of  
273 organics on pH. Recent studies indicate that organic aerosol can have a secondary, but still  
274 quantifiable impact on aerosol pH, especially when allowed to interact with inorganics (Pye et al.  
275 2018). Most 3D models do not account for potential, non-ideal interactions between the two, in  
276 addition to not including organics in thermodynamic calculations, which, if the above statement  
277 is true, can lead to significant predictive pH errors. To investigate the role of organics on pH we  
278 used the E-AIM model (Wexler & Clegg 2002, Friese & Ebel 2010, Clegg et al. 1992)  
279 (<http://www.aim.env.uea.ac.uk/aim/aim.php>) on our model results for the SEARCH sites, to  
280 calculate partitioning with organics/inorganic interactions considered. We tested a variety of  
281 organic compounds under different scenarios to determine the potential of organics to influence  
282 pH (see SI: Organic acids and pH).

283 We find that addition of organic compounds to the model, did not have a significant impact  
284 on acidity ( $\leq 2\%$  pH deviation from the baseline value) compared to the baseline run, apart from  
285 the cases where RH was higher than 80% and the mole fraction of organic acids in the aqueous  
286 phase is greater than 25% (SI: Organic acids and pH). We conclude that the maximum impact of  
287 organics on aerosol pH can likely result from the effects of liquid-liquid phase separation (Pye et  
288 al. 2018), but of insufficient magnitude to sustain a positive aerosol pH trend as observed in our  
289 basecase simulation.

## 290 **The impact of pH biases on nitrate partitioning and “sulfate-nitrate substitution”**

291 To understand the importance of pH biases on nitrate partitioning and the potential for  
292 predicting a behavior consistent with “nitrate substitution”, we express the CMAQ output in each  
293 grid cell in terms of the nitrate partitioning ratio,  $\epsilon_{NO_3} = \frac{[NO_3^-]}{[HNO_3] + [NO_3^-]}$ . It can be shown that  $\epsilon_{NO_3}$   
294 follows a simple sigmoidal curve (Meskhidze et al. 2013, Guo et al. 2016),  $\epsilon_{NO_3} = 1 - \frac{[H^+]}{[H^+] + L \cdot T \cdot \Psi}$ ,

295 where  $L$  is the liquid water content,  $T$  is ambient temperature,  $[H^+]$  is the concentration of  $H^+$  in  
 296 the aerosol aqueous phase, and  $\Psi = \frac{R \cdot [HNO_3]}{1000 \cdot P_0}$  is a fitting parameter that depends on the universal  
 297 gas constant ( $R$ ), the effective Henry's law constant for nitric acid in the aerosol aqueous phase  
 298 ( $H_{NO_3}$ ) and the ambient pressure ( $P_0$ ). Depending on the value of pH, nitrate partitioning in CMAQ  
 299 can either be insensitive ( $\frac{\partial \varepsilon_{NO_3}}{\partial pH} \sim 0$ ) or sensitive ( $\frac{\partial \varepsilon_{NO_3}}{\partial pH} \sim 0.5$ ) to pH biases, depending on the  
 300 month of the year considered (Figure 4). We generally find that nitrate partitioning is insensitive  
 301 ( $\frac{\partial \varepsilon_{NO_3}}{\partial pH} \sim 0$ ) and heavily shifted to the gas phase ( $\varepsilon_{NO_3} \sim 0$ ) during the summer and spring (Figure  
 302 4), while it becomes quite sensitive to pH errors ( $\frac{\partial \varepsilon_{NO_3}}{\partial pH} \sim 0.5$ ) in the winter and fall. For the latter  
 303 case, this means that small pH perturbations in either direction can strongly affect the amount of  
 304 nitrate that partitions in the aerosol phase; if the weather is sufficiently cold and  $NO_x$  emissions  
 305 and pH predictions are biased sufficiently high,  $\varepsilon_{NO_3} \sim 1$ , meaning that all nitrates are partitioned  
 306 to the aerosol phase and the emergence of “nitrate substitution” behavior.

307 To exemplify the above, we determine the amount of excess nitrate from pH prediction  
 308 biases as follows. Perturbing the acidity by  $\Delta pH$  from the monthly mean value along the  $\varepsilon_{NO_3}$   
 309 curves (Figure 4) gives the corresponding change in the partitioning ratio ( $\Delta \varepsilon_{NO_3}$ ). Multiplying  
 310  $\Delta \varepsilon_{NO_3}$  with the total nitrate ( $HNO_{3(g)} + NO_3$ ) predicted in CMAQ in each grid cell gives the total  
 311 nitrate response ( $\Delta NO_3$ ) to  $\Delta pH$ . When applied to the Eastern US for  $\Delta pH = +1$  (the average pH  
 312 impact of including NVCs in the  $PM_{2.5}$  calculations over the entire Eastern US) gives the  $\Delta NO_3$   
 313 distributions shown in Figure 5 for the winter (Figure 5a) and the summer (Figure 5b). The  
 314 predicted wintertime nitrate bias tends to be higher than in the summer, owing to the lower  
 315 temperatures and higher aerosol pH levels present (which shift  $\varepsilon_{NO_3}$  towards higher values; Figure  
 316 4) and the higher values of total available nitrate in the wintertime. The combination of both factors  
 317 (available nitrate and high pH) is necessary for appreciable quantities of nitrate to partition, but in  
 318 general the locations with a pH of between 0.5 and 1 are the most susceptible to positive pH biases,  
 319 since a unit increase places nitrate partitioning into the ascending part of the S-curve (Figure 4),  
 320 rapidly increasing the amount of aerosol nitrate that can form. During both seasons, areas rich in  
 321 total nitrate, and a pH between 0.5 and 1.5, such as the Ohio River Valley, New York, New Jersey  
 322 and South Louisiana (Figure 1, S1e, f), exhibit the largest increases in aerosol nitrate. Other  
 323 locations that have low pH, and low total nitrate such as West Virginia see minimal changes. A

324 notable exception is North Carolina which has a higher pH than the aforementioned locations -  
325 mainly due to the high NH<sub>3</sub> emissions from livestock - which pushes the partitioning beyond the  
326 sensitive regime, where increases in pH do not drive additional nitrate in the particle phase.

327 To investigate the potential of NVCs and sulfate reductions to induce nitrate substitution,  
328 the sensitivity of the nitrate increase  $\Delta\text{NO}_3$ , to the corresponding sulfate reduction  $\Delta\text{SO}_4$ , was  
329 quantified for the Eastern US, both when NVCs are included in the calculations and when they  
330 were not (Figure 6). Over the decade, nitrate has seen increases in the Eastern US (Figure S11)  
331 ranging from 0.5 to 2.5  $\mu\text{g m}^{-3}$ , and NVCs can have a profound impact on how these increases are  
332 distributed across the domain (Figure S11a, b). In the presence of NVCs (Figure 6a), there is a 1  
333  $\mu\text{g m}^{-3}$  increase of nitrate for a sulfate reduction of the same value over the Eastern US. For this  
334 case, substitution is predicted across the entire Eastern US, with only a few gridcells in South  
335 Georgia, Mississippi and North Carolina exhibiting the opposite trend (nitrate reduction),  
336 attributed to the formation of insoluble CaSO<sub>4</sub>, which reduces the availability of aerosol water,  
337 and in turn inhibits the formation of NO<sub>3</sub> with the co-condensation of NH<sub>3</sub>. When NVCs are  
338 removed (Figure 6b), the corresponding nitrate increase is much less (0-0.2  $\mu\text{g m}^{-3}$  per 1  $\mu\text{g m}^{-3}$  of  
339 sulfate), especially in the Eastern US, while substitution is still predicted in the Northern parts of  
340 the domain such as Ohio, Indiana and Michigan. The aforementioned areas, tend to have higher  
341 seasonal pH values than the SE US (Figure 1), and the removal of NVCs reduces the pH to values  
342 where nitrate partitioning is more sensitive to small pH perturbations (Figure 4), leading to a higher  
343 predicted sensitivity to sulfate reductions. This analysis suggests that nitrate substitution is of a  
344 much smaller magnitude than expected (West et al. 1999, Heald et al. 2012, Bauer et al. 2007,  
345 Bellouin et al. 2011, Li et al. 2011, Goto et al. 2016, Vayenas et al. 2005, Karydis et al. 2016), and  
346 heavily impacted by pH biases introduced from NVCs.

347 Given the importance of aerosol acidity for almost any aerosol-related process and impact,  
348 it is imperative that aerosol studies evaluate acidity inferred from thermodynamic analysis of  
349 ambient data as presented here. We demonstrate that in the case of nitrate substitution, the  
350 distribution of nonvolatile cations over particle size can have a profound impact on model  
351 behavior, and requires better constraints from emissions to observations (or at least appropriate  
352 sensitivity studies, such as those carried out here, to unravel the potential impact of nonvolatile  
353 cations). Understanding aerosol pH and the drivers thereof, is a powerful tool for evaluating model  
354 performance that has never been used before. Usage of molar ratios, ion balances and other

355 conceptual models of aerosol acidity (Hennigan et al. 2015, Wang et al. 2016, Silvern et al. 2017)  
356 provide limited insights in aerosol pH and should be strongly avoided to limit incorrect  
357 conclusions.

## 358 **Acknowledgments**

359 We acknowledge support from the Phillips 66 company, an EPA STAR grant and the European  
360 Research Council Consolidator Grant 726165 – PyroTRACH. Authors declare no conflict of  
361 interest. This work was funded, in part, by U.S. Environmental Protection Agency under grant  
362 RD834799. Its contents are solely the responsibility of the grantee and do not necessarily represent  
363 the official views of the US EPA. Further, the US EPA does not endorse the purchase of any  
364 commercial products or services mentioned in the publication. Observational data were provided  
365 by Atmospheric Research Associates.

## 366 **References**

- 367 Air Pollutant Emissions Trends Data, [https://www.epa.gov/air-emissions-inventories/air-](https://www.epa.gov/air-emissions-inventories/air-pollutant-emissions-trends-data)  
368 [pollutant-emissions-trends-data](https://www.epa.gov/air-emissions-inventories/air-pollutant-emissions-trends-data)
- 369 Bauer, S. E., Koch, D., Unger, N., Metzger, S. M., Shindell, D. T., and Streets, D. G.: Nitrate  
370 aerosols today and in 2030: a global simulation including aerosols and tropospheric ozone, *Atmos.*  
371 *Chem. Phys.*, 7, 5043-5059, doi:10.5194/acp-7-5043-2007, 2007.
- 372 Bellouin, N., J. Rae, A. Jones, C. Johnson, J. Haywood, and O. Boucher (2011), Aerosol forcing  
373 in the Climate Model Intercomparison Project (CMIP5) simulations by HadGEM2-ES and the role  
374 of ammonium nitrate, *J. Geophys. Res.*, 116,D20206, doi:10.1029/2011JD016074
- 375 Blanchard, C.L., Hidy, G.M., Tanenbaum, S., Edgerton, E.S. and Hartsell, B.E. 2013a. The  
376 Southeastern Aerosol Research and Characterization (SEARCH) study: Temporal trends in gas  
377 and PM concentrations and composition, 1999-2010. *J. Air Waste Manage. Assoc.*, 63:247-259.
- 378 Blanchard, C.L., Hidy, G.M., Tanenbaum, S., Edgerton, E.S. and Hartsell, B.E. 2013b. The  
379 Southeastern Aerosol Research and Characterization (SEARCH) study: Spatial variations and  
380 chemical climatology, 1999-2010. *J. Air Waste Manage. Assoc.*, 63:260-275.
- 381 Bougiatioti, A., Nikolaou, P., Stavroulas, I., Kouvarakis, G., Weber, R., Nenes, A., Kanakidou,  
382 M., and Mihalopoulos, N.: Particle water and pH in the eastern Mediterranean: source variability  
383 and implications for nutrient availability, *Atmos. Chem. Phys.*, 16, 4579-4591, doi:10.5194/acp-  
384 16-4579-2016, 2016.
- 385 Byun, D. W., and K. L. Schere, 2006: Review of the governing equations, computational  
386 algorithms, and other components of the Models-3 Community Multiscale Air Quality (CMAQ)  
387 Modeling System. *Appl. Mech. Rev.*, 59, 51-77.
- 388 Clegg, S. L., Pitzer, K. S., and Brimblecombe, P., Thermodynamics of multicomponent, miscible,  
389 ionic solutions. II. Mixtures including unsymmetrical electrolytes. *J. Phys. Chem.* 96, 9470-9479,  
390 DOI: 10.1021/j100202a074, 1992

391 Eddingsaas, N.C, VanderVelde, D.G, and Wennberg, P.O Kinetics and Products of the Acid-  
392 Catalyzed Ring-Opening of Atmospherically Relevant Butyl Epoxy Alcohols, *The Journal of*  
393 *Physical Chemistry A* 2010 114 (31), 8106-8113, DOI: 10.1021/jp103907c  
394

395 Fang, T., Guo, H., Zeng, L., Verma, V., Nenes, A., Weber, R.J. (2017) Highly acidic ambient  
396 particles, soluble metals and oxidative potential: A link between sulfate and aerosol toxicity,  
397 *Env.Sci.Tech.*, 51 (5), pp 2611–2620, doi:10.1021/acs.est.6b06151  
398

399 Fisher, J.A., D.J. Jacob, Q. Wang, R. Bahreini, C.C. Carouge, M.J. Cubison, J.E. Dibb, T. Diehl,  
400 J.L. Jimenez, E.M. Leibensperger, Z. Lu, M.B.J. Meinders, H.O.T. Pye, P.K. Quinn, S. Sharma,  
401 D.G. Streets, A. van Donkelaar, and R.M. Yantosca. 2011. "Sources, distribution, and acidity of  
402 sulfate-ammonium aerosol in the Arctic in winter-spring." *Atmospheric Environment* 45: 7301-  
403 7318.

404 Fountoukis, C. and Nenes, A. (2007) ISORROPIA II: A Computationally Efficient Aerosol  
405 Thermodynamic Equilibrium Model for  $K^+$ ,  $Ca^{2+}$ ,  $Mg^{2+}$ ,  $NH_4^+$ ,  $Na^+$ ,  $SO_4^{2-}$ ,  $NO_3^-$ ,  $Cl^-$ ,  $H_2O$   
406 Aerosols, *Atmos.Chem.Phys.*, 7, 4639–4659

407 Friese, E. and Ebel, A., Temperature dependent thermodynamic model of the system  $H^+$  -  $NH_4^+$   
408 -  $Na^+$  -  $SO_4^{2-}$  -  $NO_3^-$  -  $Cl^-$  -  $H_2O$ . *J. Phys. Chem. A*, 114, 11595-11631, DOI:  
409 10.1021/jp101041j, 2010

410 Wang, G., Zhang, R., Gomez, M. E., Yang, L., Levy Zamora, M., Hu, M., Lin, Y., Peng, J., Guo,  
411 S., Meng, J., Li, J., Cheng, C., Hu, T., Ren, Y., Wang, Y., Gao, J., Cao, J., An, Z., Zhou, W., Li,  
412 G., Wang, J., Tian, P., Marrero-Ortiz, W., Secret, J., Du, Z., Zheng, J., Shang, D., Zeng, L., Shao,  
413 M., Wang, W., Huang, Y., Wang, Y., Zhu, Y., Li, Y., Hu, J., Pan, B., Cai, L., Cheng, Y., Ji, Y.,  
414 Zhang, F., Rosenfeld, D., Liss, P. S., Duce, R. A., Kolb, C. E., and Molina, M. J.: Persistent sulfate  
415 formation from London Fog to Chinese haze, *Proc. Natl. Acad. Sci. U.S.A.*, 113, 13630-13635,  
416 doi:10.1073/pnas.1616540113, 2016.

417 Ghio, A. J., Carraway, M. S. & Madden, M. C. Composition of air pollution particles and oxidative  
418 stress in cells, tissues, and living systems. *J. Toxicol. Environ. Health B* 15, 1–21 (2012).  
419



420 Goto, D., Ueda, K., Ng, C.F.S., Takami, A., Ariga, T., Matsubishi, K., Nakajima, T., Estimation  
421 of excess mortality due to long-term exposure to PM<sub>2.5</sub> in Japan using a high-resolution model  
422 for present and future scenarios. *Atmospheric Environment* 2016;140:320–332.  
423 doi:10.1016/j.atmosenv.2016.06.015

424 Guo, H., Xu, L., Bougiatioti, A., Cerully, K. M., Capps, S. L., Hite Jr., J. R., Carlton, A. G., Lee,  
425 S.-H., Bergin, M. H., Ng, N. L., Nenes, A., and Weber, R. J.: Fine-particle water and pH in the  
426 southeastern United States, *Atmos. Chem. Phys.*, 15, 5211-5228, doi:10.5194/acp-15-5211-2015,  
427 2015

428 Guo, H., Sullivan, A.P., Campuzano-Jost, P., Schroder, J.C., Lopez-Hilfiger, F.D., Dibb, J.E.,  
429 Jimenez, J.L., Thornton, J.A, Brown, S.S., Nenes, A., and Weber, R.J. (2016) Fine particle pH and  
430 the partitioning of nitric acid during winter in the northeastern United States, *J.Geoph.Res.*, 121,  
431 doi:10.1002/2016JD025311

432 Guo, H., Nenes, A., and Weber, R. J.: The underappreciated role of nonvolatile cations on aerosol  
433 ammonium-sulfate molar ratios, *Atmos. Chem. Phys. Discuss.*, [https://doi.org/10.5194/acp-2017-](https://doi.org/10.5194/acp-2017-737)  
434 737, in review, 2017a

435 Guo, H., Liu, J., Froyd, K. D., Roberts, J. M., Veres, P. R., Hayes, P. L., Jimenez, J. L., Nenes,  
436 A., and Weber, R. J.: Fine particle pH and gas–particle phase partitioning of inorganic species in  
437 Pasadena, California, during the 2010 CalNex campaign, *Atmos. Chem. Phys.*, 17, 5703-5719,  
438 doi:10.5194/acp-17-5703-2017, 2017b

439 Guo, H., R. J. Weber, and A. Nenes, High levels of ammonia do not raise fine particle pH  
440 sufficiently to yield nitrogen oxide-dominated sulfate production, *Sci. Reports*, 7(12109),  
441 DOI:10.1038/s41598-41017-11704-41590, 2017c.

442 Hand, J. L., Schichtel, B. A., Malm, W. C., and Pitchford, M. L.: Particulate sulfate ion  
443 concentration and SO<sub>2</sub> emission trends in the United States from the early 1990s through 2010,  
444 *Atmos. Chem. Phys.*, 12, 10353-10365, doi:10.5194/acp-12-10353-2012, 2012.

445 Heald, C. L. et al. Atmospheric ammonia and particulate inorganic nitrogen over the United States.  
446 *Atmos. Chem. Phys.* 12, 10295–10312 (2012).

447 Henneman, L.R.F., Liu, C., Hu, Y., Mulholland, J.A., Russell, A.G. (2017), “Air quality modeling  
448 for accountability research: Operational, dynamic, and diagnostic evaluation.”, *Atm.Env.*, 166,  
449 551–565

450 Hennigan, C. J., Izumi, J., Sullivan, A. P., Weber, R. J., and Nenes, A.: A critical evaluation of  
451 proxy methods used to estimate the acidity of atmospheric particles, *Atmos. Chem. Phys.*, 15,  
452 2775-2790, doi:10.5194/acp-15-2775-2015, 2015.

453 Karydis, V. A., Tsimpidi, A. P., Pozzer, A., Astitha, M., and Lelieveld, J.: Effects of mineral dust  
454 on global atmospheric nitrate concentrations, *Atmos. Chem. Phys.*, 16, 1491-1509,  
455 doi:10.5194/acp-16-1491-2016, 2016.

456 Kim, P. S., Jacob, D. J., Fisher, J. A., Travis, K., Yu, K., Zhu, L., Yantosca, R. M., Sulprizio, M.  
457 P., Jimenez, J. L., Campuzano-Jost, P., Froyd, K. D., Liao, J., Hair, J. W., Fenn, M. A., Butler, C.  
458 F., Wagner, N. L., Gordon, T. D., Welti, A., Wennberg, P. O., Crounse, J. D., St. Clair, J. M.,  
459 Teng, A. P., Millet, D. B., Schwarz, J. P., Markovic, M. Z., and Perring, A. E.: Sources,  
460 seasonality, and trends of southeast US aerosol: an integrated analysis of surface, aircraft, and  
461 satellite observations with the GEOS-Chem chemical transport model, *Atmos. Chem. Phys.*, 15,  
462 10411-10433, doi:10.5194/acp-15-10411-2015, 2015.

463 Laskin, A., R. C. Moffet, M. K. Gilles, J. D. Fast, R. A. Zaveri, B. B. Wang, P. Nigge, and J.  
464 Shutthanandan (2012), Tropospheric chemistry of internally mixed sea salt and organic particles:  
465 Surprising reactivity of NaCl with weak organic acids, *Journal Of Geophysical Research-*  
466 *Atmospheres*, 117, D017743.

467

468 Liu, M., Song, Y., Zhou, T., Xu, Z., Yan, C., Zheng, M., Wu, Z., Hu, M., Wu, Y., and Zhu, T.:  
469 Fine particle pH during severe haze episodes in northern China, *Geophys. Res. Lett.*, 44, 5213-  
470 5221, doi:10.1002/2017GL073210, 2017

471

472 Li, J., W.-C. Wang, H. Liao, and W. Chang. 2014. Past and future direct radiative forcing of nitrate  
473 aerosol in East Asia. *Theor. Appl. Climatol.* 1–14. doi:10.1007/s00704-014-1249-1

474 Liu, Y., Wu Z., Wang, Y., Xiao, Y., Gu, F., Zheng, J., Tan, T, Shang, D., Wu, Y., Zeng, L., Hu,  
475 M., Bateman, A. P., and Martin, S.T., Submicrometer Particles Are in the Liquid State during  
476 Heavy Haze Episodes in the Urban Atmosphere of Beijing, China, *Environmental Science &*  
477 *Technology Letters Article ASAP*, DOI: 10.1021/acs.estlett.7b00352, 2017

478 Meskhidze, N., Chameides, W. L., Nenes, A. & Chen, G. Iron mobilization in mineral dust: can  
479 anthropogenic SO<sub>2</sub> emissions affect ocean productivity? *Geophys. Res. Lett.* 30, 2085 (2003).

480 Park, R. J., Jacob, D. J., Kumar, N. and Yantosca, R. N.. 2006. Regional visibility statistics in the  
481 United States: Natural and transboundary pollution influences, and implications for the regional  
482 haze rule. *Atmospheric Environment* 40(28): 5405-5423,  
483 doi.org/10.1016/j.atmosenv.2006.04.059

484 Pinder, R. W., Adams, P. J. & Pandis, S. N. Ammonia emission controls as a cost-effective strategy  
485 for reducing atmospheric particulate matter in the eastern United States. *Environ. Sci. Technol.*  
486 41, 380–386 (2007).

487 Pinder, R. W., Gilliland, A. B. & Dennis, R. L. Environmental impact of atmospheric NH<sub>3</sub>  
488 emissions under present and future conditions in the eastern United States. *Geophys. Res. Lett.*  
489 35, L12808 (2008).

490 Pye, H. O. T., H. Liao, S. Wu, L. J. Mickley, D. J. Jacob, D. K. Henze, and J. H. Seinfeld (2009),  
491 Effect of changes in climate and emissions on future sulfate-nitrate-ammonium aerosol levels in  
492 the United States, *J. Geophys. Res.*, 114, D01205, doi:10.1029/2008JD010701.

493 Pye, H. O. T., Zuend, A., Fry, J. L., Isaacman-VanWertz, G., Capps, S. L., Appel, K. W., Foroutan,  
494 H., Xu, L., Ng, N. L., and Goldstein, A. H.: Coupling of organic and inorganic aerosol systems  
495 and the effect on gas–particle partitioning in the southeastern US, *Atmos. Chem. Phys.*, 18, 357-  
496 370, <https://doi.org/10.5194/acp-18-357-2018>, 2018.

497 Pye, H. O. T.; Pinder, R. W.; Piletic, I. R.; Xie, Y.; Capps, S. L.; Lin, Y.-H.<sup>S</sup>; Surratt, J. D.; Zhang,  
498 Z.; Gold, A.; Luecken, D. J.; Hutzell, W. T.; Jaoui, M.; Offenberg, J. H.; Kleindienst, T. E.;  
499 Lewandowski, M.; Edney, E. O. (2013) Epoxide Pathways Improve Model Predictions of Isoprene

500 Markers and Reveal Key Role of Acidity in Aerosol Formation. *Environmental Science &*  
501 *Technology*, 47 (19), 11056–11064.

502 Saylor, R., Myles, L., Sibble, D., Caldwell, J. & Xing, J. Recent trends in gas-phase ammonia and  
503 PM<sub>2.5</sub> ammonium in the southeast United States. *J. Air Waste Manage. Assoc.* 65, 347–357, doi:  
504 10.1080/10962247.2014.992554, 2015

505 Silvern, R. F., Jacob, D. J., Kim, P. S., Marais, E. A., Turner, J. R., Campuzano-Jost, P., and  
506 Jimenez, J. L.: Inconsistency of ammonium–sulfate aerosol ratios with thermodynamic models in  
507 the eastern US: a possible role of organic aerosol, *Atmos. Chem. Phys.*, 17, 5107–5118,  
508 doi:10.5194/acp-17-5107-2017, 2017.

509 Song, S., Gao, M., Xu, W., Shao, J., Shi, G., Wang, S., Wang, Y., Sun, Y., and McElroy, M. B.:  
510 Fine particle pH for Beijing winter haze as inferred from different thermodynamic equilibrium  
511 models, *Atmos. Chem. Phys. Discuss.*, <https://doi.org/10.5194/acp-2018-6>, in review, 2018.

512 Surratt, J. D., Chan, A. W. H., Eddingsaas, N. C., Chan, M., Loza, C. L., Kwan, A. J., Hersey, S.  
513 P., Flagan, R. C., Wennberg, P. O., and Seinfeld, J. H.: Reactive intermediates revealed in  
514 secondary organic aerosol formation from isoprene, *P. Natl. Acad. Sci. USA*, 107, 6640–6645,  
515 doi:10.1073/pnas.0911114107, 2010.

516

517 Tsimpidi, A. P., Karydis, V. A. & Pandis, S. N. Response of inorganic fine particulate matter to  
518 emission changes of sulfur dioxide and ammonia: the eastern United States as a case study. *J. Air*  
519 *Waste Manage. Assoc.* 57, 1489–1498 (2007).

520 Vayenas, D. V., S. Takahama, C. I. Davidson, and S. N. Pandis (2005), Simulation of the  
521 thermodynamics and removal processes in the sulfate-ammonia-nitric acid system during winter:  
522 Implications for PM<sub>2.5</sub> control strategies, *J. Geophys. Res.*, 110, D07S14,  
523 doi:10.1029/2004JD005038.

524 Weber, R.J., Guo, H., Russell, A.G., Nenes, A. (2016) High aerosol acidity despite declining  
525 atmospheric sulfate concentrations over the past 15 years, *Nature Geosci.*, doi:10.1038/ngeo2665

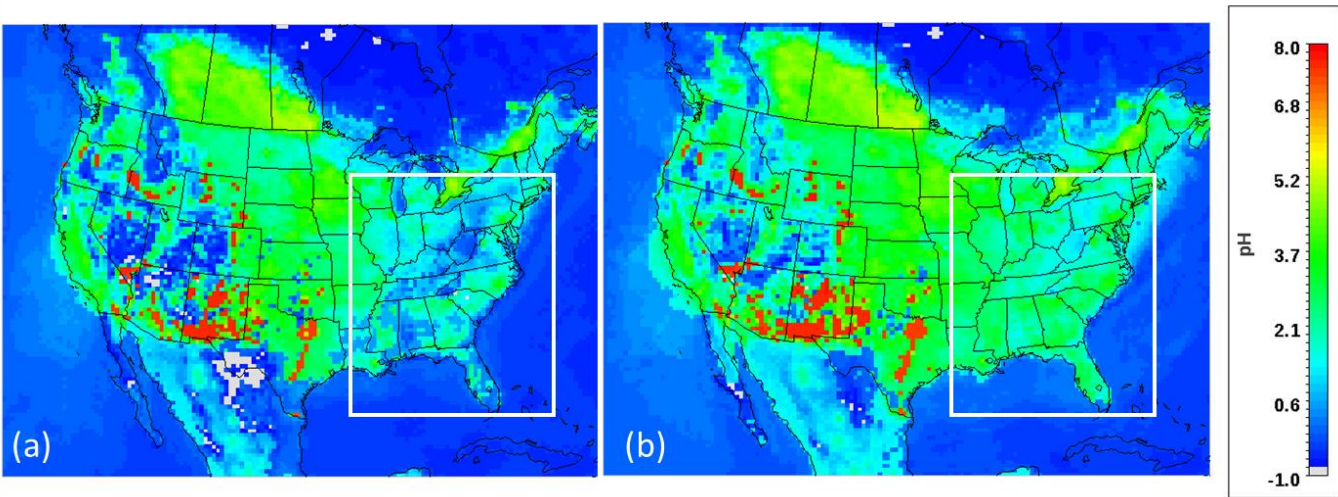
526 Li, W., Xu, L., Liu, X., Zhang, J., Lin, Y., Yao, X., Gao, H., Zhang, D., Chen, J., Wang, W.,  
527 Harrison, R., Zhang, X., Shao, L., Fu, P., Nenes, A., Shi, Z. Air pollution–aerosol interactions  
528 produce more bioavailable iron for ocean ecosystems. *Science Advances*, 2017; 3 (3): e1601749  
529 DOI: 10.1126/sciadv.1601749

530 West, J. J., Ansari, A. S. & Pandis, S. N. Marginal PM<sub>2.5</sub>: nonlinear aerosol mass response to  
531 sulfate reductions in the eastern United States. *J. Air Waste Manage. Assoc.* 49, 1415–1424  
532 (1999).

533 Wexler, A. S., and S. L. Clegg, Atmospheric aerosol models for systems including the ions H<sup>+</sup>,  
534 NH<sub>4</sub><sup>+</sup>, Na<sup>+</sup>, SO<sub>4</sub><sup>2-</sup>, NO<sub>3</sub><sup>-</sup>, Cl<sup>-</sup>, Br<sup>-</sup>, and H<sub>2</sub>O, *J. Geophys. Res.*, 107(D14), DOI:  
535 10.1029/2001JD000451, 2002, <http://www.aim.env.uea.ac.uk/aim/aim.php>

536 Xu, L.; Guo, H.; Boyd, C.; Klein, M.; Bougiatioti, A.; Cerully, K.; Hite, J.; Isaacman-VanWertz,  
537 G.; Kreisberg, N. M.; Knote, C.; Olson, K.; Koss, A.; Goldstein, A.; Hering, S. V.; de Gouw, J.;  
538 Baumann, K.; Lee, S. H.; Nenes, A.; Weber, R. J.; Ng, N. L. Effects of anthropogenic emissions  
539 on aerosol formation from isoprene and monoterpenes in the southeastern United States. *Proc.*  
540 *Natl. Acad. Sci. U. S. A.* 2014, 112 (1), 37–42.

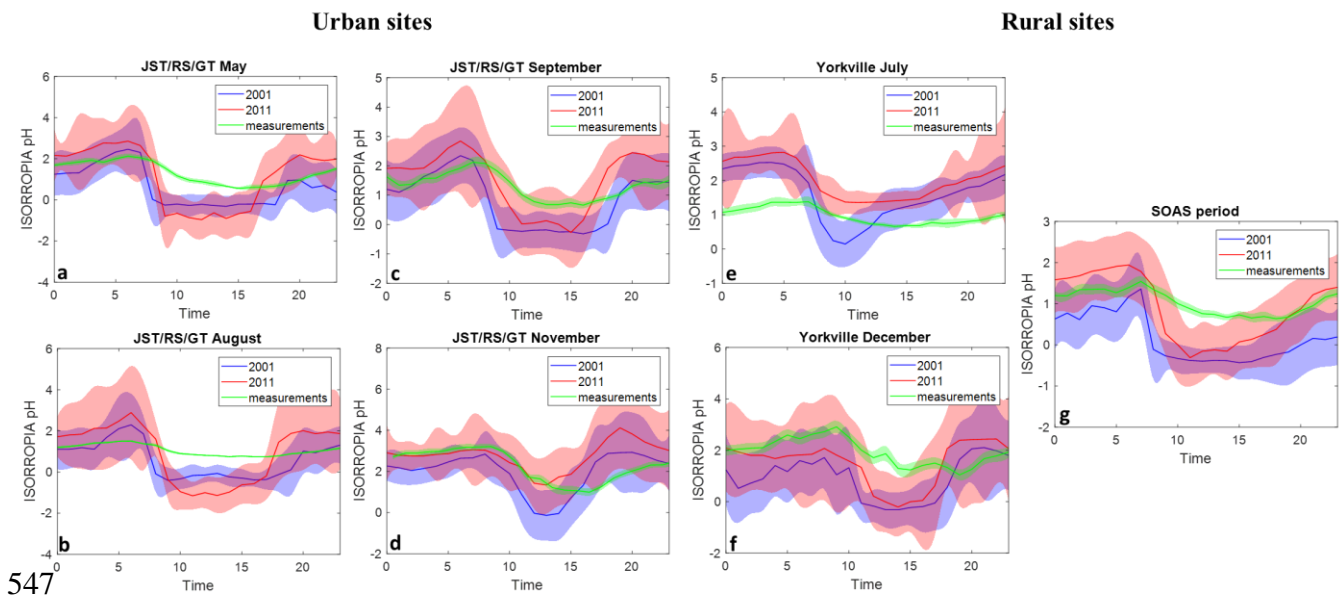
541



542

543 **Figure 1** - Annual averaged PM<sub>2.5</sub> pH over CONUS for (a) 2001 and (b) 2011, calculated offline  
544 using ISORROPIA, using the annual averaged CMAQ concentration fields. The white outline  
545 specifies the Eastern US domain used for further analysis.

546

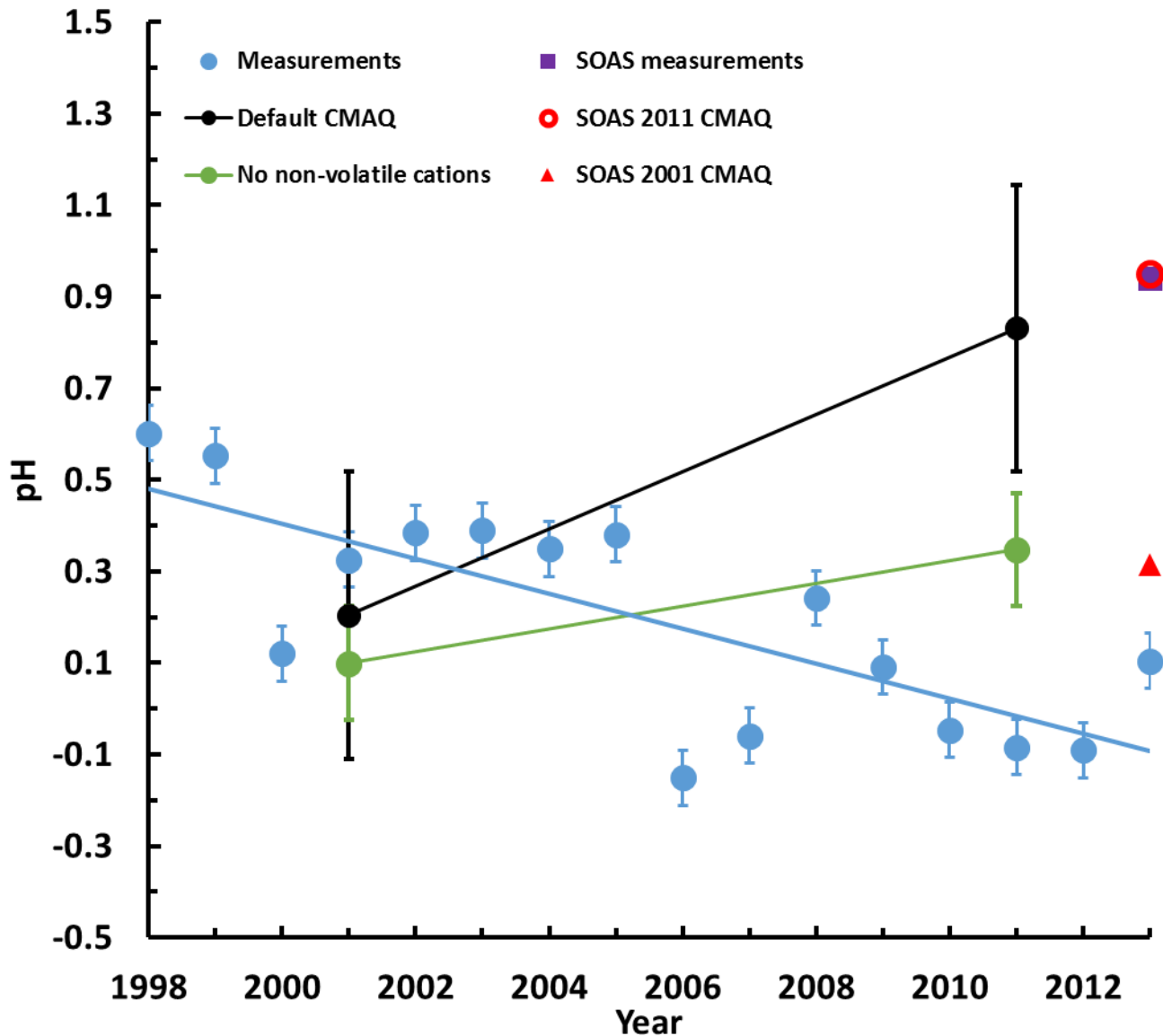


547

548

549 **Figure 2** - pH diurnal profiles for May (a), August (b), September (c) and November (d) at  
 550 JST/RS/GT, July (e) and December (f) at YRK and for the SOAS campaign period (g). Blue and  
 551 red lines are the offline ISORROPIA simulated pH using CMAQ concentrations for 2001 and  
 552 2011 respectively, while the shaded areas are one model standard deviation. The green line  
 553 represents the pH calculated through the thermodynamic analysis of the measurements (found in

554 Guo et al., 2015) and the shaded area is standard standard error

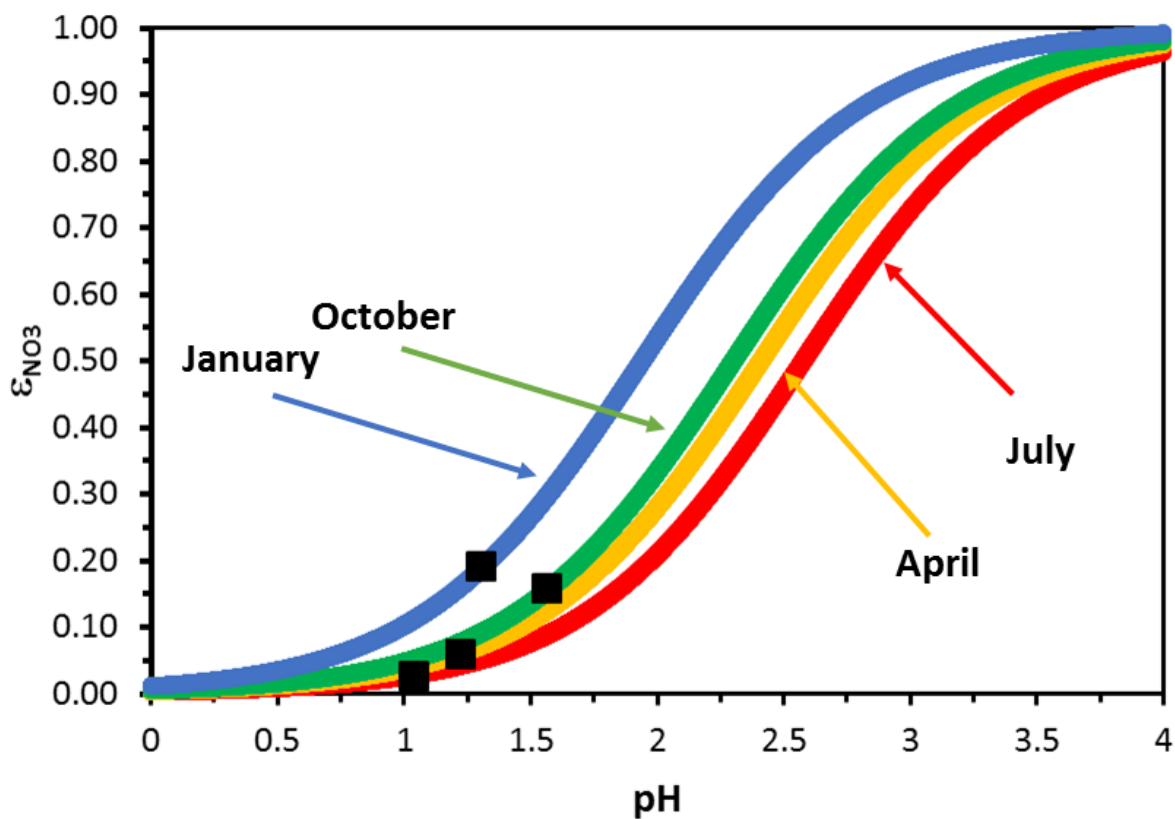


555  
556 **Figure 3** – Decadal pH trends from the thermodynamic analysis of the measurements from Weber  
557 et al. 2016 (blue line), default CMAQ (black line) and CMAQ results at the Centreville gridcell  
558 without crustal elements (green line). Also shown, is the pH for the SOAS campaign, and for the  
559 CMAQ predicted pH for June 1<sup>st</sup>-July 15<sup>th</sup> 2001 and 2011. CMAQ exhibits a clear positive trend,  
560 with pH increasing throughout the decade, both due to sulfate reductions and the increasingly  
561 important role of NVCs. Standard error is also plotted for all data points.

562

563

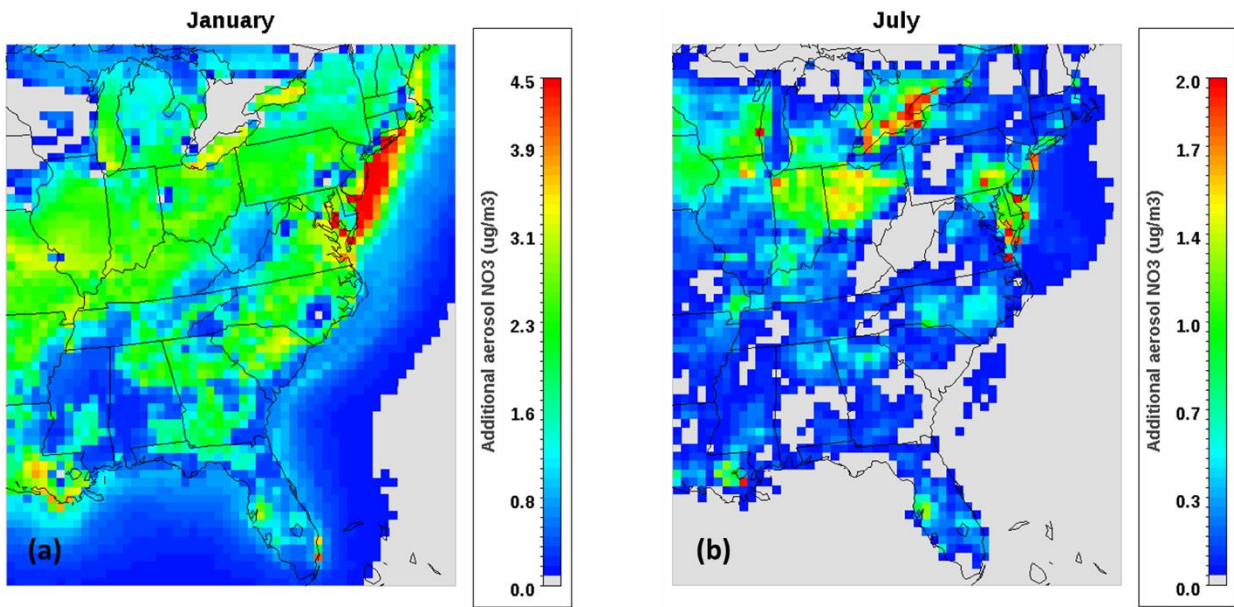




564  
 565 **Figure 4** - CMAQ-derived nitrate partitioning ratio for the E.U.S. and select months of 2001. The  
 566 black squares denote the average pH values for each month. Note the insensitivity of nitrate  
 567 partitioning to pH biases in the summer for pH values of less than 1 ( $\frac{\partial \epsilon_{NO_3}}{\partial pH} \sim 0$ ), which is not the case  
 568 for colder months.

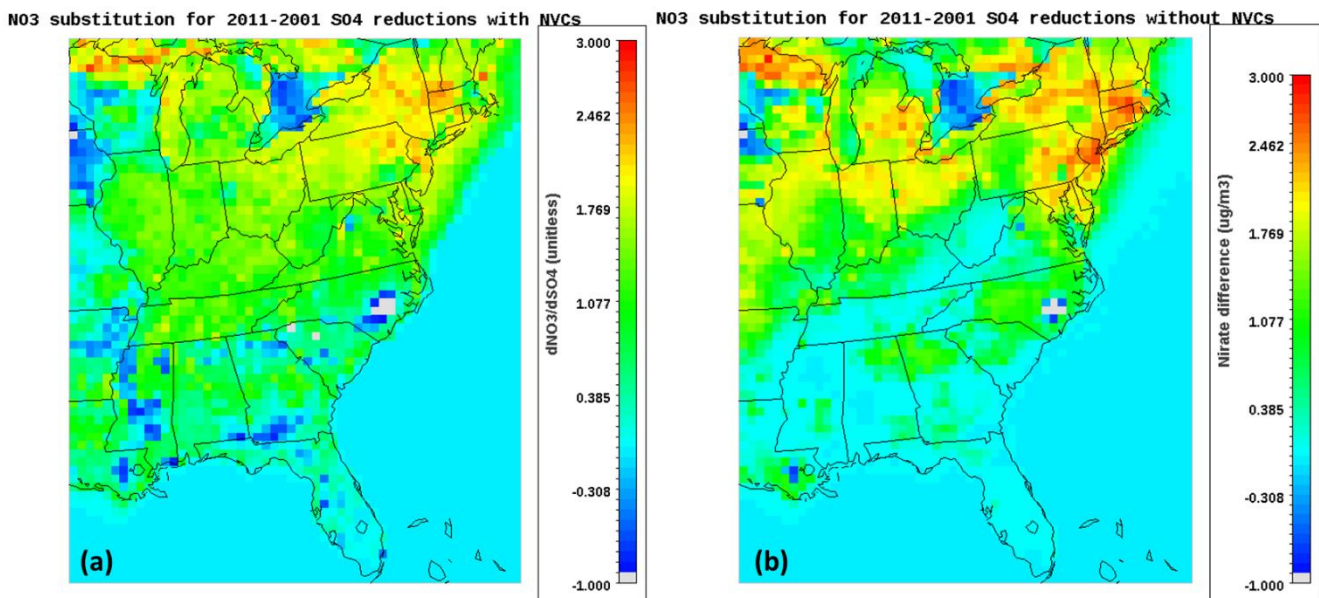
569

570



571

572 **Figure 5** - Increase in aerosol nitrate corresponding to a one-unit positive change in pH for a)  
573 January and b) July. Emissions for 2011 are assumed, but to account for pH prediction biases from  
574 NVCs, they are removed from the thermodynamic calculations. Plots are on different scales due  
575 to the large differences in predicted nitrate increases.



576

577 **Figure 6** – CMAQ predicted nitrate substitution  $\left(\frac{NO_3^{2011}-NO_3^{2001}}{SO_4^{2001}-SO_4^{2011}}\right)$  over the decade, when NVCs  
578 are accounted for (a), and when they are removed from the thermodynamic calculations (b).